Pergamon

Cement and Concrete Research, Vol. 28, No. 6, pp. 815–828, 1998

0008-8846/98 $19.00 + .00

PII S0008-8846(98)00061-1

STUDY OF THE RELATION BETWEEN HYDRATED PORTLAND CEMENT COMPOSITION AND LEACHING RESISTANCE

R.J. van Eijk[1] and H.J.H. Brouwers
Department of Civil Engineering & Management, University of Twente, P.O. Box 217, 7500 AE Enschede, The Netherlands

(Received October 13, 1997; in final form April 15, 1998)

ABSTRACT

The present paper addresses cement compositions that have an optimal resistance against acid attack and hence, low leaching rates and optimal waste containment. To this end a shrinking core leaching model is used that describes the leaching of metals from a cement sample. This process is directly related to the calcium hydroxide removal from the sample by the acidified leachant. Effective diffusion coefficients in this so-called leached shell were calculated using the equations derived from a cement hydration model. This results in equations in which leaching rates were dependent on cement composition, especially the calcium hydroxide fraction. Optimizing the calcium hydroxide fraction yields cement compositions possessing the optimal leaching resistance as a function of the water porosity or as a function of the hydration degree and water to cement ratio used. The results were also used for the determination of optimal amounts of silica fume and fly ash. A comparison with experimental and practical data reported in literature yields good agreement. © *1998 Elsevier Science Ltd*

Introduction

Portland cement can be combined with wastes in order to prevent leaching of species such as heavy metals into the environment. This technique is referred to as immobilization or stabilization/solidification (S/S). The ability of cement with respect to fixing hazardous components and prevention of leaching lies in both the physical and chemical properties of the matrix. In leaching tests, cement specimens are subjected to acidified water for prescribed time periods after which metal concentrations in the leachant are measured. In the U.S., the TCLP (1) and ANS/ANSI 16.1 (2) prescribe the execution of such tests, whereas in The Netherlands recently, NEN 7343 (3) and NEN 7345 (4) have been introduced as regulatory tests.

In the past, efforts have been made in order to model the leaching from immobilisates and predict leaching test results. Godbee and Joy (5) used a semi-infinite medium diffusion model and obtained an expression for the leaching from monoliths. Based on the same bulk

[1]To whom correspondence should be addressed.

diffusion model, Brouwers (6) derived an expression for the leaching of granular materials. The bulk diffusion model however does not account for the leachant pH nor the observed matrix dissolution taking place in the cement during exposure to an acidic environment (7,8). During this process the portlandite (or $Ca(OH)_2$, in cement chemistry notation: CH) present in the cement matrix dissolves. This results in the presence of an unaltered shrinking core and a moving leached shell in which the CH is removed (9,10). Cheng and Bishop (11) found that in the leached shell stabilized metals were removed while metal concentrations in the core were still unchanged. Hinsenveld and Bishop (12) presented a shrinking core model which describes the transport of species by diffusion through this leached shell.

The presence of CH in the cement matrix is of major importance for the leaching. First, this component acts as acid buffer for the acidified water that enters the matrix and releases the contaminants. On the other hand, after dissolution the removed CH generates extra porosity facilitating transport of species by diffusion through the leached shell and resulting in an increasing progress of the dissolution front in the matrix.

Equations for the computation of cement-gel fraction (in cement chemistry notation: CSH), water fraction (or porosity), and CH fractions as function of the water/cement ratio were derived from the cement hydration model developed by Bentz and Garboczi (13). Furthermore, they simulated CH leaching using their model and derived an expression for the effective diffusion coefficient in a cement matrix during the leaching process (14,15). This effective diffusion coefficient mainly depends on the porosity of the matrix, and was in accordance with experimental data (16). Their objective however, was limited to reducing the porosity below the critical value where porosity is not connected anymore. However, the positive effect of the CH phase when it acts as buffering barrier against the acid attack was not considered.

In this paper, the results of the mentioned cement hydration model will be used to predict leaching rates as described by the model of Hinsenveld and Bishop (12). Combining the analytical expressions yield an optimal composition of hydrated cement and w/c ratio that minimizes the leaching rate of the sample. It is believed that this information is of major importance in predicting regulatory test results and creating cement matrices that are effective in containing hazardous contaminants. Subsequently, the analytical predictions are compared with experimental results provided by the literature. Finally, the positive effect of adding pozzolanic admixtures such as silica fume and fly ash is analyzed in some detail.

Implementation of Matrix Composition into Leaching Model

Following the shrinking core model, the cumulative amount leached per unit exposed surface area can be calculated as follows (12,17):

$$M(t) = \sqrt{\frac{2 \cdot D_e \cdot C_0^{\,2} \cdot f_{mo}^{\,2} \cdot C_H}{\beta}} \cdot \sqrt{t} \tag{1}$$

where $M(t)$ is the cumulative amount leached contaminant per unit exposed surface area [mol/m^2], D_e is the effective diffusion coefficient [m^2/s], C_0 is the initial metal concentration in sample [mol/m^3], f_{mo} is the mobile fraction of metal, C_H is the H^+ concentration in leachant [mol/m^3], β is the acid neutralization capacity (ANC) [mol/m^3], and t is time [s].

As can be seen from Eq. 1, the release rate depends both on the effective diffusion

coefficient of the contaminant species in the leached shell and the acid buffering capacity of the cement specimen.

In the present analysis, it is assumed that the acid buffering capacity of cement is directly related to the amount of free calcium present in cement. This calcium originates from both the CH and cement hydrate (in cement chemistry notation: CSH). In a leached shell, CH is considered completely dissolved and contributes directly to the ANC, where each mol of CH directly contributes 1 mol of Ca^{2+}.

CSH also contributes to the ANC, but diffusion of calcium from CSH is less complete and much slower than dissolution of CH (18–21). Revertegate et al. (18) performed experiments in which OPC cement samples (w/c ratio 0.37) were immersed in water at different pH values. After certain periods the samples were analyzed: the total calcium content was determined by XRF, while CH was analyzed by thermogravimetry. In this way they were able to separate the leaching of calcium from CH and CSH phases. At pH 4.6, all CH dissolved and 68% of the CSH calcium was dissolved. This agrees fairly well with results of Carde et al. (19) who measured calcium profiles of cement samples with and without CH after chemical attack by ammonium nitrate. They observed that the CSH phase had a linear decalcification profile from the surface of the sample to the end of the degraded zone, while decalcification of the CH phase in this zone was complete. For the samples without CH they found a 50% decalcification of the CSH in the degraded zone. Considering these experiments an average decalcification value of 0.6 for the CSH will be used in this analysis.

The short-hand notation CSH in fact stands for $C_{1.7}SH_4$ (22). This means that 1 mol of CSH can release 1.7 mol Ca^{2+}. Using the given molar volumes of 33.1×10^{-3} L/mol and 108×10^{-3} L/mol for CH and CSH, respectively (22,23), and the fact that every Ca^{2+} ion is capable of consuming two H^+, the equation for the ANC finally takes the following form:

$$\beta = 2\cdot\frac{\varphi_{CH}}{33.1\cdot10^{-3}\left[\frac{l}{mol}\right]} + 2\cdot0.6\cdot1.7\cdot\frac{\varphi_{CSH}}{108\cdot10^{-3}\left[\frac{l}{mol}\right]} = (60.4\cdot\varphi_{CH} + 18.9\cdot\varphi_{CSH})\left[\frac{mol}{l}\right] \quad (2)$$

where φ_{CH} is the CH volume fraction and φ_{CSH} is the CSH volume fraction.

Next, the effective diffusion coefficient of H^+ appearing in Eq. 1 is related to the porosity of the leached shell. Garboczi and Bentz (15) derived an equation in which the relative diffusion coefficient of a species in a cement matrix is related to the porosity as follows:

$$\frac{D_e}{D_0} = 0.001 + 0.07\varphi_w^2 + H(\varphi_w - 0.18)\cdot1.8\cdot(\varphi_w - 0.18)^2 \quad (3)$$

where φ_w is the water porosity, $H(x)$ is 0 when $x \leq 0$, $H(x)$ is 1 when $x > 0$, and D_0 is the molecular diffusion coefficient.

The reciprocal of the left-hand side of Eq. 3 is referred to as MacMullin number (24), which depends on the structure of the cement matrix only, whereas H is the Heaviside function. The value of 0.18 is called the percolation threshold (14).

Equation 3 holds for a standard unleached cement matrix. During leaching, however, CH in the sample is dissolved, resulting in extra porosity. The total porosity in a leached sample, φ_t, therefore exists of both initial (or water) porosity, φ_w, and a porosity fraction originating from the CH fraction, φ_{CH}, that was present before leaching:

$$\varphi_t = \varphi_w + \varphi_{CH} \quad (4)$$

where φ_t is the total porosity (porosity after leaching) and φ_w is the water porosity (porosity before leaching).

Unfortunately, Eq. 3 does not hold during leaching because the diffusivity increases much more rapidly during leaching compared to the decrease in diffusivity during hydration (14,25). This means that for a certain porosity the diffusivity in a leached sample is higher than in the unleached form and cannot be derived by simply substituting φ_t into Eq. 3. Snyder and Clifton (25) developed equations that take this effect into account. They defined the following functions ϑ_w and ϑ_t as the results of substituting φ_w and φ_t respectively into Eq. 3:

$$\vartheta_w = 0.001 + 0.07\varphi_w^2 + H(\varphi_w - 0.18)\cdot 1.8\cdot(\varphi_w - 0.18)^2 \quad (5)$$

$$\vartheta_t = 0.001 + 0.07\varphi_t^2 + H(\varphi_t - 0.16)\cdot 1.8\cdot(\varphi_t - 0.16)^2 \quad (6)$$

Using these expressions, the relative diffusion coefficient in a leached sample was calculated as follows:

$$\frac{D_e}{D_0} = 2\vartheta_t - \vartheta_w \quad (7)$$

As indicated by Eq. 6, during leaching a percolation threshold of 0.16 is used instead of 0.18 (14). Therefore, this value should be used for calculating ϑ_t for a leached sample while 0.18 is appropriate for calculating ϑ_w of the original sample. Using these two different percolation thresholds, the relative diffusion coefficient can now be calculated according to Eq. 7. The first term of the final equation however should be a cut-off value in case both φ_w and φ_t tend to zero. A value of 0.001 is considered an appropriate mean value for samples that contain a certain amount of CH. However, in a leached shell that consists purely of CSH and does not contain CH anymore, a cut-off value of 0.0025 should be used, which is the relative diffusion coefficient for the CSH phase. Combining all equations now yields:

$$\frac{D_e}{D_0} = 0.0025 - 0.07\varphi_w^2 - H(\varphi_w - 0.18)\cdot 1.8\cdot(\varphi_w - 0.18)^2 + 0.14\varphi_t^2 + H(\varphi_t - 0.16)\cdot 3.6\cdot(\varphi_t - 0.16)^2 \quad (8)$$

As can be concluded from the previous analysis, the φ_{CH} fraction has two opposite effects on the metal release rate during acid attack, namely: 1) a positive effect by increasing acid buffering capacity; and 2) a negative effect by increasing porosity in the leached shell, thereby increasing the effective diffusion coefficient.

This means that the cement composition can be optimized by varying this variable in order to obtain an optimal resistance against acid attack. To this end, using Eqs. 2 and 8, Eq. 1 is rewritten as:

$$\frac{M(t)}{\sqrt{2\cdot C_0^2\cdot f_{mo}^2\cdot C_H\cdot D_0}} = f(\varphi_{CH}, \varphi_W, \varphi_{CSH}) = \sqrt{\frac{0.0025 - 0.07\varphi_w^2 - H(\varphi_w - 0.18)\cdot 1.8\cdot(\varphi_w - 0.18)^2 + 0.14\varphi_t^2 + H(\varphi_t - 0.16)\cdot 3.6\cdot(\varphi_t - 0.16)^2}{60.4\cdot\varphi_{CH} + 18.9\cdot\varphi_{CSH}}} \quad (9)$$

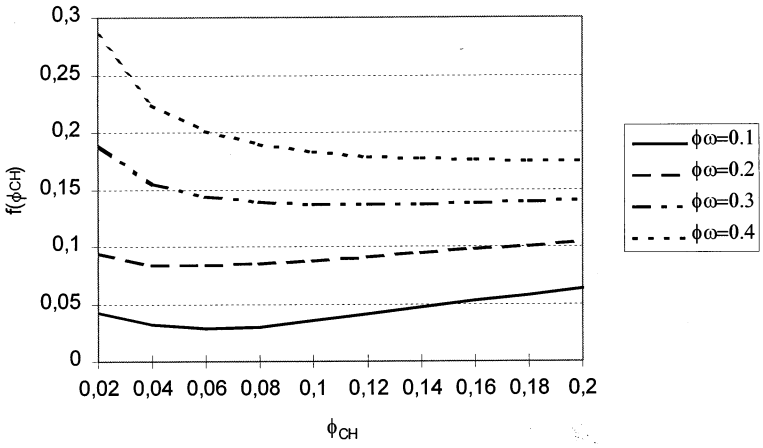

FIG. 1.
$f(\varphi_{CH})$ plotted for various water porosity fractions φ_w.

Note that the right-hand side solely depends on the cement composition, while the left-hand side contains all contaminant properties.

The cement hydration model of Bentz and Garboczi (14) was originally based on the hydration of C_3S only and the corresponding volume stoichiometries of this reaction as determined by Young and Hansen (22). Many studies revealed this hydration to be representative for the hydration of OPC (ordinary Portland cement). In later work (23), saturated curing and chemical shrinkage were implemented into this model and the following volume stoichiometry was found to give the best model results:

$$C_3S \rightarrow 1.52\ CSH + 0.61\ CH \tag{10}$$

Using Eq. 10 as a simplified description for the hydration of OPC and assuming that no silica is present the amounts of CSH and CH can be directly related to each other as follows:

$$\varphi_{CSH} = 2.5 \cdot \varphi_{CH} \tag{11}$$

and Eq. 2 then becomes:

$$\beta = 107.6 \varphi_{CH} \left[\frac{mol}{l} \right] \tag{12}$$

Inserting Eq. 11 into Eq. 9, one obtains a function $f(\varphi_{CH}, \varphi_w)$ that describes leaching rate:

$$\frac{M(t)}{\sqrt{2 \cdot C_0^{\,2} \cdot f_{mo}^{\,2} \cdot C_H \cdot D_0}} = f(\varphi_{CH}, \varphi_W) = \sqrt{\frac{0.0025 - 0.07\varphi_W^{\,2} - H(\varphi_w - 0.18) \cdot 1.8 \cdot (\varphi_w - 0.18)^2 + 0.14\varphi_t^{\,2} + H(\varphi_t - 0.16) \cdot 3.6 \cdot (\varphi_t - 0.16)^2}{107.6 \cdot \varphi_{CH}}} \tag{13}$$

In Figure 1, this function $f(\varphi_{CH}, \varphi_w)$ is drawn vs. φ_{CH} for various values of φ_w.

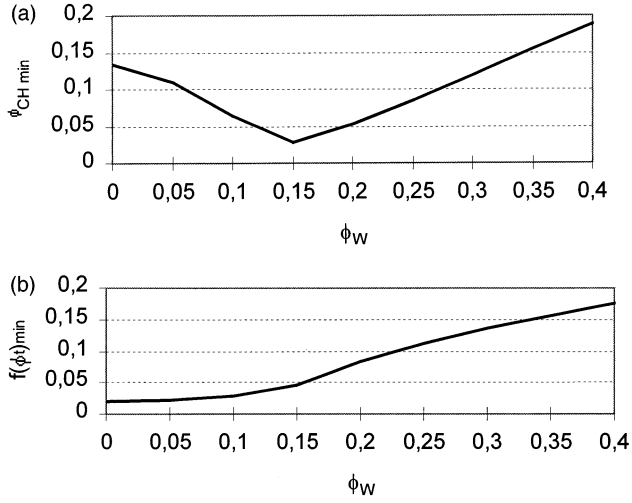

FIG. 2.

A) φ_{CH} for which $f(\varphi_t)$ is minimal ($\varphi_{CH\ min}$) plotted for various values of φ_w. *B*) Minimum $f(\varphi_t)$ plotted against φ_w.

One can see from Figure 1 that for each φ_w, a φ_{CH} exists for which $f(\varphi_{CH}, \varphi_w)$ is minimal. Figure 1 also shows that the positive dependency on φ_{CH} of the function f is more pronounced at low water porosities, and the negative dependency on φ_{CH} is more pronounced at high water porosities. As expected, for every φ_{CH}, f is lowest when φ_w is lowest.

The φ_{CH} for which $f(\varphi_{CH}, \varphi_w)$ is minimal, denoted as $\varphi_{CH\ min}$, follows from differentiating the right-hand side of Eq. 13 with respect to φ_{CH}:

$$\frac{df(\varphi_{CH}, \varphi_w)}{d\varphi_{CH}} = \frac{1}{2f} \cdot \frac{0.14\varphi_{CH}^2 + H(\varphi_W - 0.18)\cdot 1.8\cdot(\varphi_w - 0.18)^2 - 0.0025 - 0.07\varphi_w^2}{\varphi_{CH}^2} + \frac{1}{2f} \cdot \frac{H(\varphi_t - 0.16)\cdot 3.6\cdot(\varphi_{CH}^2 - \varphi_w^2 + 0.32\varphi_w - (0.16)^2)}{\varphi_{CH}^2} \tag{14}$$

Setting the right-hand side equal to zero yields:

$$\varphi_{CH} = \sqrt{0.5\varphi_w^2 + 0.0178} \qquad \text{for } \varphi_w < 0.16,\ \varphi_t < 0.16 \tag{15}$$

$$\varphi_{CH} = \sqrt{0.98\varphi_w^2 - 0.308\varphi_w + 0.025} \qquad \text{for } \varphi_w < 0.18,\ \varphi_t > 0.16 \tag{16}$$

$$\varphi_{CH} = \sqrt{0.5\varphi_w^2 - 0.135\varphi_w + 0.0097} \qquad \text{for } \varphi_w > 0.18,\ \varphi_t > 0.18 \tag{17}$$

In Figure 2a, this $\varphi_{CH\ min}$ is plotted for different values of φ_w. In Figure 2b, the corresponding $f(\varphi_t)$ minima, denoted as f_{min} are plotted vs. φ_w.

The shape of Figure 2a again shows the dual effect of φ_{CH}. At high water porosity, when water porosity increases, φ_{CH} must also increase in order to keep f minimal. At low water porosity however, φ_{CH} must decrease as in that case φ_{CH} also has an increasing effect on f. From Figure 2b the major effect of φ_w on f_{min} is illustrated. From Figure 2a and 2b one can conclude that $f(\varphi_{CH}, \varphi_w)$ is lowest if φ_w equals zero and φ_{CH} is about 0.13.

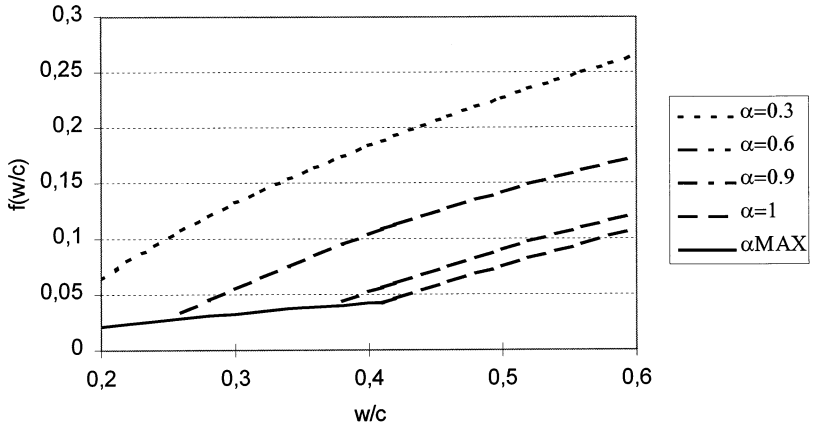

FIG. 3.
f(w/c) plotted against w/c for various α.

Calculation of Optimal w/c Ratio

In the previous section, φ_{CH} and φ_w have been treated as independent variables. These properties can, however, be related using the equation for C_3S hydration used by Bentz (23), which was given in Eq. 10 and their typical specific gravity of 3.2 kg/dm^3 for cement. Using this information from their model, the φ_{CH} and φ_w can be described as a function of the degree of hydration (α) and water/cement ratio (w/c) as follows:

$$\varphi_{CH} = \frac{0.191\alpha}{w/c + 0.313} \tag{18}$$

$$\varphi_w = \frac{w/c - 0.410\alpha}{w/c + 0.313} \tag{19}$$

and hence,

$$\varphi_t = \varphi_{CH} + \varphi_w = \frac{w/c - 0.219\alpha}{w/c + 0.313} \tag{20}$$

where φ_t is the total porosity fraction, φ_{CH} is the $Ca(OH)_2$ fraction, φ_w is the water porosity fraction, w/c is the water/cement ratio, and α is the hydration degree.

Both fractions φ_{CH} and φ_w can be substituted into Eq. 13, yielding *f* as a function of w/c and α. In Figure 3, *f*(w/c) is depicted for various α, namely $\alpha = 0.30$, 0.60, 0.90, and 1. Considering that $\alpha \leq$ w/c ratio/0.41, for every w/c ratio < 0.41, hydration cannot be attained completely ($\alpha = 1$). Hence, in this case there is a maximum achievable α, depicted as α_{max}. For w/c > 0.41, hydration can proceed until $\alpha_{max} = 1$. The function $f(\alpha_{max})$ is also drawn in Figure 3. As both time and hydration proceed, for each w/c ratio the function *f* decreases until the lines corresponding to α_{max} or $\alpha = 1$ are attained. One can readily see that for practical purposes w/c ratio should be as low as possible. At low w/c ratio however, the differences in lowest achievable *f* values are very small with *f* ranging from about 0.025 to 0.05 for w/c ratio ranging from 0.2 to 0.41, respectively. Therefore, using a w/c ratio < 0.41

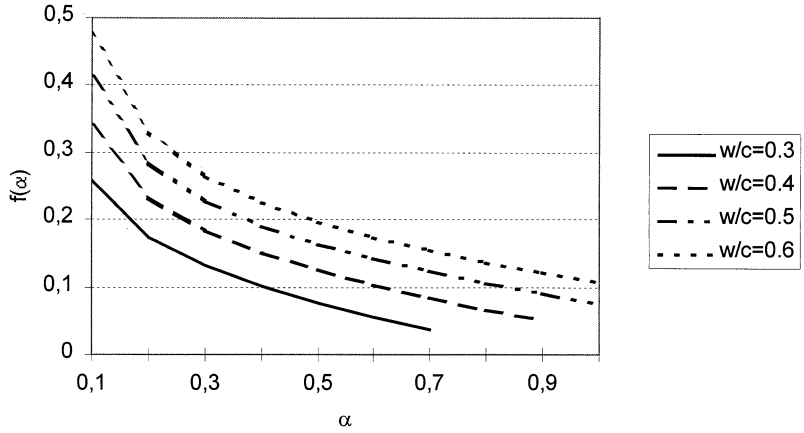

FIG. 4.
$f(\alpha)$ plotted against α for various w/c.

will be of no use in practice as it does not result in a substantial decrease in f anymore. Moreover, unhydrated cement will then remain, being unused for binding and immobilization.

In Figure 4, $f(\alpha)$ is depicted for various w/c ratio, namely w/c = 0.3, 0.4, 0.5, and 0.6 for $\alpha = 0$ until $\alpha = \alpha_{max}$. From this figure it is clear that f decreases during hydration. One may also conclude from Figure 4 that using a higher w/c ratio can only result in a lower f value when hydration degree is significantly higher. At complete hydration a higher w/c ratio will always result in a higher leaching rate.

Comparison with Experiments

In the previous section, a theoretical model has been presented for the leaching from hydrated cement matrices. In this section, the theoretical predictions are compared with some experimental data obtained from the literature.

Zamorani and Serrini (26) performed leaching experiments on Cs^+-ions immobilized in cement samples at different w/c values. Ordinary Portland cement was used and all samples were cured at 60°C, 98% R.H. for 11 days. The samples were leached in water at a surface-to-liquid volume of 0.1/cm. It was found that the cumulative fraction leached (CFR) depends on both $\sqrt{t}$, which is in qualitative agreement with Eq. 1, and the w/c ratio. C_0, f_{mo}, C_H, and D_0 can be assumed constant for each of their experiments and were calibrated using their results for w/c = 0.4. The CFR can now be related to f via:

$$\frac{CFR}{CFR_{wcf=0.4}} = \frac{f}{f(\text{w/c} = 0.4)} \tag{21}$$

Densities and total pore volumes of all samples are given by the reference in [g/cm^3] and [cm^3/g], respectively. In order to obtain the water porosity fractions φ_w for each sample, the given total pore volumes in [cm^3/g] were multiplied with the measured and reported sample densities. These resulting water porosity fractions were then used to estimate the hydration

TABLE 1
f ratios compared to CFR ratios (Zamorano and Serrini, 1992).

wcf	estimated α	$CFR/CFR_{w/c=0.4}$	$f/f(w/c = 0.4)$
0.35	0.49	0.89	0.89
0.4	0.53	1	1
0.45	0.52	1.24	1.19
0.5	0.65	1.36	1.25

degree α of every sample using the relation between these two as given in Eq. 19. Using this estimated hydration degree α, *f* was calculated for each w/c ratio used in the experiments.

In Table 1, the calculated *f* ratios are compared with CFR ratios for various w/c ratio. One can readily conclude that the agreement between experiments and the here presented model predictions are good, especially when one considers the simplifications invoked in the present analysis. This implies that the combination of leaching model and cement composition, resulting in the function *f*, adequately describes the leaching process as a function of cement composition.

Addition of Pozzolanic Admixtures

Silica fume, a highly reactive amorphous silica material, can be used as an admixture. It reacts with the CH released during hydration and forms CSH. A typical density of 2.2 kg/dm^3 for silica will be used. Two situations should be considered when silica (in cement chemistry notation: S) is present:

1. All CH produced during hydration of the cement is consumed by the initial amount of S, forming CSH. This implies that some unreacted silica remains in the hydrated sample, while $\varphi_{CH} = 0$. The relevant volume fractions can be calculated as follows (14):

$$\varphi_{CSH} = \frac{2.868\alpha(1 - m)}{3.2\cdot(w/s + 0.14m) + 1} \tag{22}$$

$$\varphi_S = \frac{1.45m - 0.293\alpha(1 - m)}{3.2\cdot(w/s + 0.14m) + 1} \tag{23}$$

and

$$\varphi_w = 1 - \frac{(1 + 1.755\alpha)(1 - m) + 1.45m}{3.2\cdot(w/s + 0.14m) + 1} \tag{24}$$

where w/s is the water/solid ratio (i.e., cement and silica fume), m is the silica fume mass/cement and silica fume mass, and φ_S is the S volume fraction.

By definition the w/s ratio and the w/c ratio can be related to each other as follows:

$$w/s = (1 - m)\cdot w/c \tag{25}$$

The corresponding silica fume volume fraction *x* can be related to the mass fraction *m* as follows (14):

$$x = \frac{3.2m}{2.2(1-m) + 3.2m} \tag{26}$$

where 3.2 and 2.2 are typical densities in kg/dm^3 for cement and pozzolanic admixtures respectively.

2. More CH is produced during hydration than can be consumed by the initial amount of S. This situation occurs when the amount of CH produced is higher than the amount of CH consumed, which means that (14):

$$0.61(1-x)\alpha > 2.08x \tag{27}$$

or

$$m \leq \frac{\alpha}{\alpha + 4.96} \tag{28}$$

where 0.61 is the amount of CH produced by one volume element of C_3S and 2.08 is the amount of CH consumed by one volume element of S (or pozzolanic reactivity factor).

When the silica fume fraction fulfills condition (27), a CH fraction will remain in the final sample and all volume fractions of interest can be calculated as follows (14):

$$\varphi_{CSH} = \frac{1.52\alpha(1-m) + 6.67m}{3.2\cdot(w/s + 0.14m) + 1} \tag{29}$$

$$\varphi_{CH} = \frac{0.61\alpha(1-m) - 3m}{3.2\cdot(w/s + 0.14m) + 1} \tag{30}$$

and

$$\varphi_{w} = 1 - \frac{(1 + 1.31\alpha)(1-m) + 3.67m}{3.2\cdot(wsf + 0.14m) + 1} \tag{31}$$

In the presence of silica fume, the amounts of CSH and CH are no longer related by Eq. 11. Therefore the simplified Eq. 12 for the ANC is not valid anymore and Eq. 2 should be used instead, in which φ_{CSH} and φ_{CH} are calculated separately in order to obtain the ANC. Using the *f* function from Eq. 9 and Eqs. 29–31 for all volume fractions, *f*(*m*) can be calculated for samples with silica fume. In Figure 5, the function *f*(*m*) is plotted for various w/s, namely 0.35, 0.40, and 0.5. α was taken as 0.7, which means that, according to Eq. 27, when $m > 0.12$, $\varphi_{CH} = 0$ and silica remains in the sample.

The amount of S is optimal when *f* is as low as possible, but it should be noted that also S as such should be as low as possible, considering its high price. From Figure 5 it can be seen that such optima exist. Silica replaces CH with CSH in a sample. Because calcium is more strongly bound in CSH compared to CH this calcium contributes less to the ANC (see also Eq. 2). In other words, the replacement of CH for CSH makes the calcium less available for buffering. As from the point where all CH is consumed, the addition of more silica still has a negative effect on the ANC because then it replaces cement and less CSH is formed during hydration. Low amounts of silica have a negative effect on total porosity during the leaching process, because less CH is leached out. However at the point where silica remains, higher amounts of silica only acts as inert filler, replacing the initial amount of cement and

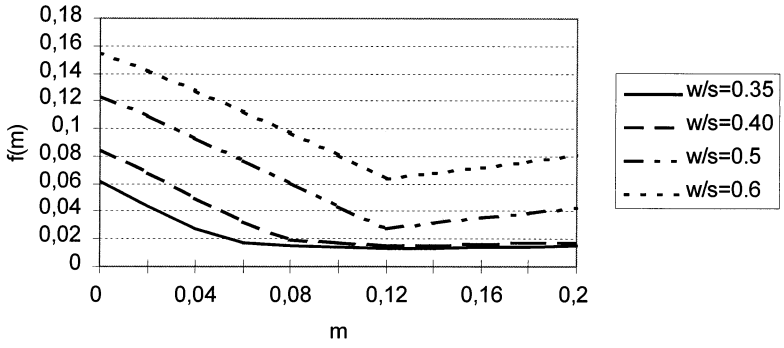

FIG. 5.
$f(m)$ plotted against silica fume mass fraction m for various w/s ($\alpha = 0.7$).

increasing the final water porosity. These effects are responsible for the shape of the plots in Figure 5. The minima in these plots correspond to the point where all CH is consumed because at that point both water and total porosities are minimal. This optimum can therefore be determined straightforward using Eq. 28. In this case, when $\alpha = 0.7$, the silica fume mass fraction where $f(m)$ is minimal is $m = 0.12$. From Figure 5, one can also see that for w/s $<$ 0.5 adding more than 8 mass % silica fume is not effective anymore.

In Figure 6, $f(m)$ is plotted for various α. The w/s was taken as 0.4. As can be seen from Figure 6 low $f(m)$ values are only possible at high hydration rates and the minima are different for all considered α. The line $\alpha = 0.9$ ends at 8 mass % silica fume because this hydration degree is not achievable anymore for samples that contain more silica fume.

From both figures it can be concluded that in general, for all w/s and α values used here, optimal silica fume contents vary between 8 and 10 mass % when α ranges from 0.3 to 0.6, respectively. For low w/s or high hydration degrees the addition of 8 mass % silica fume would be the most appropriate in theory.

Fly ash is commonly used as an admixture in waste stabilization because of its pozzolanic properties and low price. The composition of fly ash varies greatly but the amount of SiO_2 is typically 50%. Compared to the fine silica fume, fly ash has a higher particle size and was

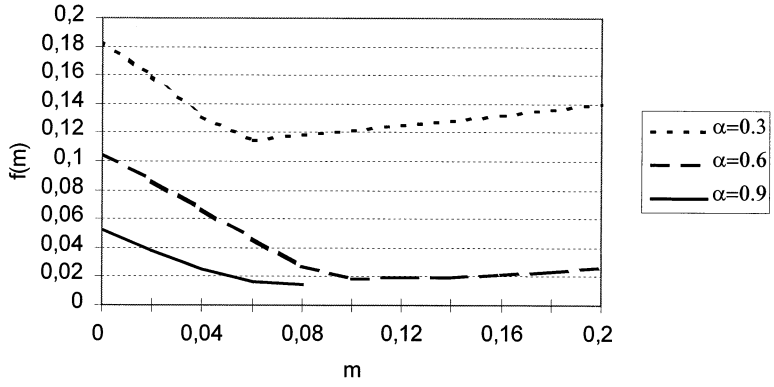

FIG. 6.
$f(x)$ plotted against silica fume mass fraction m for various α (w/s = 0.4).

found to hydrate for only 50%. Considering these typical values this would result in a pozzolanic reactivity and corresponding CH reduction of about 25% compared to silica fume. This CH reduction was observed in OPC containing 25 volume % of fly ash (27). Therefore a pozzolanic reactivity factor of 0.5 can be used for fly ash in order to account for both its lower amount of SiO_2 and its lower hydration rate compared to silica fume. Using a typical density of 2.2 kg/dm^3, the corresponding equations for fly ash can be derived in the same way as for silica fume taking into account that one volume element of fly ash now consumes 0.5 CH instead of the 2.08 volume elements of CH that were consumed by pure S.

In case of remaining fly ash and $\phi_{CH} = 0$, Eq. 22 does not change and the constants -0.293 and 1.755 in the numerators of Eqs. 23 and 24 change into -1.22 and 0.828, respectively. In the case where all fly ash has reacted, the constants 6.67, -3, and 3.67 in the numerators of Eqs. 29–31 change into 1.67, -0.725, and 0.945, respectively. Performing the same analysis as was performed in the case of silica fume, one can conclude that fly ash should be added in such an amount that all CH is consumed. Replacing the value of 2.08 for 0.5 in Eq. 27 results in Eq. 32, which is fulfilled when all CH is consumed by a certain amount of fly ash and can be used straightforward for the determination of the optimal amount of fly ash needed:

$$m_{fa} = \frac{\alpha}{\alpha + 1.24} \tag{32}$$

where m_{fa} is the fly ash mass/cement and fly ash mass.

This means that for a typical hydration degree $\alpha = 0.7$, the optimal amount of fly ash would be 36 mass % based on total mass of solids.

It should be noted that for both the values of silica fume and fly ash as theoretically determined here, are indeed also used and found effective in the field of waste immobilization (28).

Conclusions

Leaching of metals in a solidified cement sample as a result of an acid attack can be described by a shrinking core leaching model. Both the effective diffusion coefficient and the acid neutralization capacity can be described in terms of cement phase fractions. Using the leaching model and a cement hydration model, it is possible to describe leaching rates as a function of cement paste composition. When the water porosity fraction is known a CH fraction can be calculated at which leaching rates are minimal.

Because the water porosity only has a negative effect, it should always be as low as possible. Cement composition should therefore be optimized for the amount of CH. Best results are obtained when water porosity is 0% and CH fraction is 13%.

Leaching rates can also be determined as function of the w/c ratio and α, using a simplified cement hydration model that describes all phase fractions as a function of these properties. From this it follows that minimal leaching rates can only be obtained at very low w/c ratio. Furthermore, the results from the theoretical model presented here are in good agreement with the experimental data of Zamorani and Serrini (26) (see Table 1).

In order to use all cement, additions such as silica fume or fly ash are needed. The optimal replacement fractions for these pozzolanic admixtures particularly depend on the expected hydration degree α and less on the w/c ratio used. Optimal values of around 8 mass % (silica

fume) and 35 mass % (fly ash) based on total mass of cement and admixtures were calculated. This is in close agreement with the additions that are actually used in (S/S) technology. The theoretical concepts introduced here will contribute to the understanding of the relation between cement composition and leaching resistance and its effects on durability of the solidified product. Moreover, in case of the application of non standard OPC as solidifying agent, a similar analysis as executed here can be recommended and will help to find theoretical optima.

References

1. U.S. EPA, TCLP, Solid waste procedure manual, SW-924, Cincinnati (1985).
2. ANSI/ANS 16.1, Measurement of the leachability of solidified low-level radioactive wastes by a short term test procedure, American Nuclear Society, La Grange Park (1986).
3. NEN 7343, Leaching characteristics of solid earthy and stony building and waste materials, determination of the leaching of inorganic components from granular materials with the column test, Nederlands Normalisatie Instituut, Delft (in Dutch) (1995).
4. NEN 7345, Leaching characteristics of solid earthy and stony building and waste materials, Determination of the leaching of inorganic components from buildings and monolithic waste materials with the diffusion test, Nederlands Normalisatie Instituut, Delft (in Dutch) (1995).
5. H.W. Godbee and D.S. Joy, Assessment of the Loss of Radioactive Isotopes from Waste Solids to the Environment, Part 1, Background and Theory, Oak Ridge National Laboratory ORNL/TM-4333, Oak Ridge, TN, 1974.
6. H.J.H. Brouwers, J. Hazard. Mat. 53, 1–17 (1997).
7. N.I. Fattuhi and B.P. Hughes, Cem. Concr. Res. 18, 545–553 (1988).
8. K.Y. Cheng, Controlling mechanisms of metal release from cement-based waste forms in acetic acid solution, PhD Thesis, University of Cincinatti, 1991.
9. K.Y. Cheng, P. Bishop, and J. Isenburg, J. Hazard. Mat. 30, 285–295 (1992).
10. K.Y. Cheng, P. Bishop and J. Isenburg, Cement stabilization/solidification techniques: pH profile within acid-attacked waste form. Waste Materials in Construction, J.J.J.R. Goumans, H.A. van der Sloot, and Th.G. Aalbers, (eds.), Elsevier Science Publishers, New York, 1991.
11. K.Y. Cheng and P. Bishop, Hazard. Waste Hazard. Mat. 9, 163–171 (1992).
12. M. Hinsenveld and P.L. Bishop, Use of the shrinking core/exposure model to describe the leachability from cement stabilized wastes. Stabilization and solidification of hazardous, radioactive and mixed wastes, ASTM STP 1240, M. Gilliam, and C.C. Wiles, (eds.), Am. Soc. of Testing and Mat., Philadelphia, 1994.
13. D.P. Bentz and E.J. Garboczi, Ceramic Transactions 16, 211–226 (1991).
14. D.P. Bentz and E.J. Garboczi, Mater. Struct. 25, 523–533 (1992).
15. E.J. Garboczi and D.P. Bentz, J. Mater. Sci. 27, 2083–2092 (1992).
16. B.J. Christensen, T.O. Mason, H.M. Jenning, D.P. Bentz, and E.J. Garboczi, Mat. Res. Soc. Symp. Proc. 245, 259–264 (1992).
17. P.G. Baker and P.L. Bishop, J. Hazard. Mat. 52, 311–333 (1997).
18. E. Revertegate, C. Richet and P. Gegout, Cem. Concr. Res. 22, 259–272 (1992).
19. C. Carde, R. Francois, and J.-M. Torrentini, Cem. Concr. Res. 26, 1257–1268 (1996).
20. P. Faucon, P. Le Bescop, F. Adenot, P. Bonville, J.F. Jacquinot, F. Pineau, and B. Felix, Cem. Concr. Res. 26, 1707–1715 (1996).
21. M. Buil, E. Revertegat, and J.A. Oliver, A model of the attack of pure water or undersaturated lime solutions on cement, Stab. Solid. Hazard. Radioact. Wastes, 2nd Vol. STP 1123, T.M. Gilliam, and C.C. Wiles, (eds.), ASTM, Philadelphia, pp. 217–226, 1992.
22. J.F. Young and W. Hansen, Mat. Res. Soc. Symp. Proc. 85, 313–322 (1987).

23. D.P. Bentz, J. Am. Ceram. Soc. 80, 3–21 (1997).
24. A.A. Kyi and B. Batchelor, Cem. Concr. Res. 24, 752–764 (1994).
25. K.A. Snyder and J.R. Clifton, 4sight manual: A computer program for modelling degradation of underground low level waste concrete vaults, NISTIR 5612, U.S. Dept. of Commerce (1995).
26. E. Zamorani and G. Serrini, Effect of hydrating water on the physical characteristics and the diffusion release of cesium nitrate immoblized, Cement Stab. Solid. Hazard. Radioact. Wastes, 2nd Vol. STP 1123, T.M. Gilliam and C.C. Wiles (eds.), ASTM, Philadelphia, pp. 217–226, 1992.
27. R.D. Hooton, Permeability and pore structure of cement pastes containing fly ash, slag and silica fume blended cements, ASTM STP 897, G. Frohnsdorff (ed.), ASTM, Philadelphia, pp. 128–143, 1986.
28. F.P. Glasser, Waste Management 16, 159–168 (1996).